Inclusive Scattering from Nuclei at $x > 1$ and High Q^2 with a 6 GeV Beam

J. Arrington (Spokesperson), D. F. Geesaman, K. Hafidi, R. Holt, H. E. Jackson,
P. E. Reimer, E. C. Schulte
Argonne National Laboratory

B.W. Filippone (Spokesperson), R.D. McKeown
California Institute of Technology

O.K. Baker, E. Christy, L. Colt, A. Gasparian, C. Jackson, C.E. Keppel,
L. Tang, L. Yuan
Hampton University

R. Carlini, R. Ent, H. Fenker, A. Lung (Spokesperson), D. Mack, M. Jones, G. Smith,
S. Wood, W. Vulcan, C. Yan
Thomas Jefferson National Accelerator Facility

C. Carasco, M. Hauger, J. Jourdan, D. Rohe, I. Sick, G. Warren
University of Basel

D. Crabb, D.B. Day (Spokesperson), R.L. Lindgren, P. McKee, Y. Prok,
O. Rondon-Aramayo, F. Wesselmann, M. Zeier, H. Zhu
University of Virginia

(December 3, 2001)

We propose an extension to Jefferson Lab Experiment E89-008, an inclusive electron-nucleus scattering experiment in the domain of large x and Q^2. Additional measurements with a 6 GeV beam would allow study of the scaling behavior at large Q^2 and provide important constraints on the components of the nuclear wave function at large momentum and removal energy. Measurements with few-body nuclei (^{2}H, ^{3}He, and ^{4}He) and a range of heavy nuclei (C, Cu, and Au) allow contact with theoretical calculations via essentially "exact" calculations for few-body systems and extrapolation of the heavier systems to potentially calculable nuclear matter. In addition, direct comparisons of heavy nuclei to deuterium and ^{3}He at large x will allow us to examine the nature of the short range correlations that generate the high momentum nucleons.

I. INTRODUCTION

This proposal requests time to make inclusive electron scattering measurements with both few-body nuclei and heavy nuclei at high momentum transfers. Measurements at large x are sensitive to high momentum nucleons in the nucleus (momenta in excess of 1000 MeV/c for the kinematics of this proposal), and provide clean information on the high momentum components of the spectral function. The measurements with few-body nuclei allow comparisons with essentially exact calculations of nuclear wave functions and provide an important complement to the coincidence $A(e,e'p)$ and $A(e,e'NN)$ measurements already completed or approved. The measurements with heavy nuclei should allow extrapolation to nuclear matter where again rigorous calculations can be performed and compared to the data. In addition to using the data to directly constrain the spectral function at very high momenta, we will use the nuclear dependence of the cross section to study the nature of the short range correlations that are the main source of the high momentum nucleons. By comparing the distribution of high momentum nucleons in heavy nuclei to those measured in ^{2}H we can look for signatures of NN short range correlations in a model independent way. The inclusion of ^{3}He and ^{4}He measurements will also allow us to look for contributions from multinucleon short range correlations.

In addition to the main goal of studying nucleon distributions and short range correlations in nuclei, this data will allow us to extract the nuclear structure functions at large x values. This will allow us to extend measurements of duality and scaling in nuclei, which are related to the connection between the quark and hadronic pictures of nuclear structure. This experiment will also provide the data necessary to make precision measurements of the QCD moments in nuclei.

A. Connection to Deep Inelastic Scattering (DIS)

The response of the nucleus in the range $x > 1$ is expected to be composed of both deep-inelastic scattering from quarks in the nucleus and elastic scattering from the bound nucleons (quasielastic scattering). For both the bound quark and bound nucleon cases it is the non-zero momentum of the bound nucleons that permits scattering into a kinematic region that is forbidden for the free nucleon. The scattering from quarks should exhibit scaling in the Bjorken x variable (experimentally verified for $x < 1$), while the scattering from the nucleons exhibits y scaling (discussed below). However the respective scaling functions for the two processes appear to be dramatically different. It is the inclusive structure functions (*e.g.* νW_2^A) that scale for the quark case while it is the cross section weighted by the elastic form factors [$G_E(Q^2)$ and $G_M(Q^2)$] that exhibits scaling for the nucleon case. In a simple impulse approximation (Quark-Parton model for quark scattering, quasielastic (QE) nucleon scattering for the nucleon scattering) the DIS scaling functions are related to the *quark* momentum distributions in the nucleus, while the quasielastic scaling function is related to the *nucleon* momentum distributions. It is the weighting by the elastic form factors, which fall with a high power of Q^2, that causes the quasielastic response to vanish in the limit of $Q^2 \to \infty$. In this limit the deep inelastic scattering from quarks should dominate the response even for $x > 1$. Thus the two types of scaling appear to be significantly different. A possible connection between the two has been suggested in several analyses of the previous data [1–3]. Here the nuclear structure function is taken versus the Nachtmann scaling variable ξ, and an interesting scaling (for all ξ) is suggested by the data [4] (Fig. 1). ξ is a modified version of the deep inelastic scaling variable ($\xi \to x$ as $Q^2 \to \infty$) that takes into account target mass effects and thus reduces scaling violations at finite Q^2 values. The Q^2 range of the previous SLAC data was too limited to draw firm conclusions about the nature of this scaling. One theoretical analysis [5] suggested that the observed scaling is accidental and would break down at larger Q^2. A more recent work [6] explains ξ-scaling as an approximation to scaling in ξ_{QE}, which is analogous to ξ but describes scattering from quasifree nucleons in the nucleus. For both of these explanations, the scaling in ξ is described as an approximation to scaling for quasielastic scattering, where scaling violations coming from the transformation from y (ξ_{QE}) to ξ are either small or cancelled by other contributions. However, in the kinematics covered by the previous JLab experiment with a 4 GeV beam, the scaling violations that come from the change of scaling variables are much larger than the observed scaling violations [4].

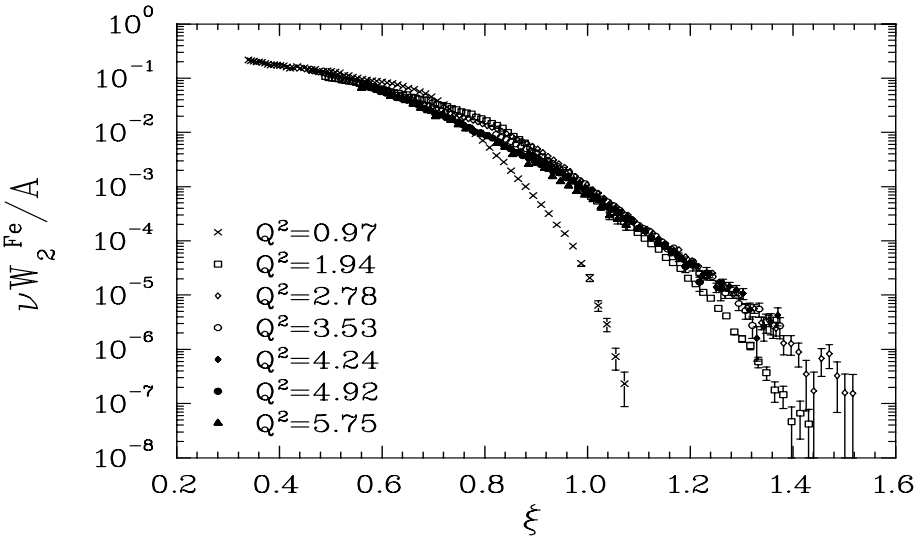

FIG. 1. Structure function per nucleon for Fe vs. the Nachtmann scaling variable from Jefferson Lab E89-008. The Q^2 values are given for Bjorken $x = 1$. Errors shown are statistical only.

The connection between the inelastic and quasielastic regions seems to be a consequence of duality, as observed first by Bloom and Gilman [7], and studied more precisely in recent Jefferson Lab experiments [8]. In the proton, it was observed that the resonance region structure function, *averaged over the resonances*, is identical to the DIS structure function. In the nucleus, the Fermi motion of the nucleons performs this averaging and duality yields true scaling, rather than scaling on average, in regions where the intrinsic averaging is sufficient. While this explains the scaling in the resonance region, it is not clear why the scaling works so well for $\xi > 1$, where at moderate Q^2 we are sensitive only to the quasielastic contributions, and where we average only over part of the quasielastic peak.

In addition to providing information about the scaling behavior at $x > 1$, these measurements provide the necessary data to perform precise moment analyses of nuclei. Current moment analyses are limited at moderate to high Q^2 values by the knowledge of the structure function at $x > 1$, especially for the higher moments. Combining this data with lower x measurements from duality studies of hydrogen and deuterium [9,10] and other planned measurements of light nuclei [11] will allow a more precise determination of the first several moments of the nuclear structure function. A comparison of the moments of deuterium and hydrogen may allow a determination of the moments for the neutron without some of the theoretical ambiguities that arise when attempting to directly extract the neutron structure function from data on nuclei.

Exploring the transition from Quasielastic scaling (*i.e.* y-scaling) to DIS scaling (x-scaling) requires measurements at the highest possible Q^2. Measurements with a 6 GeV beam will significantly extend the accessible Q^2 range compared to what is possible with a 4 GeV beam. Comparisons of deuterium and heavy nuclei at $x > 1$ for high Q^2 allows one to study scattering from high momentum partons, as well as allowing searches for modifications of quark distributions due to the nuclear medium in a new kinematic regime.

B. High Momentum Components in the Nucleus

High energy electron scattering from nuclei can provide important information on the wave function of nucleons in the nucleus. With simple assumptions about the reaction mechanism, scaling functions can be deduced that should scale (*i.e.* become independent of length scale or momentum transfer) and which are directly related to the momentum distribution of nucleons in a nucleus. Several theoretical studies [12–15] have indicated that such measurements may provide direct access to short range nucleon-nucleon correlations.

The concept of y-scaling in electron-nucleus scattering was first introduced by West [16] and by Kawazoe *et al.* [17]. They showed that in the impulse approximation, if quasielastic scattering from a nucleon in the nucleus was the dominant reaction mechanism, a scaling function $F(y)$ could be extracted from the measured cross section which was related to the momentum distribution of the nucleons in the nucleus. In the simplest approximation the corresponding scaling variable y is the minimum momentum of the struck nucleon along the direction of the virtual photon. The scaling function is defined as the ratio of the measured cross section to the off-shell electron-nucleon cross section multiplied by a kinematic factor:

$$F(y) = \frac{d^2\sigma}{d\Omega d\nu} \frac{1}{(Z\sigma_p + N\sigma_n)} \frac{q}{\sqrt{(M^2 + (y+q)^2)}}, \tag{1}$$

where Z and N are the number of protons and neutrons in the target nucleus, the off-shell cross sections σ_p and σ_n are taken from σ_{CC1} from Ref. [18], q is the three-momentum transfer and M is the mass of the proton. At large q, where we can neglect momenta perpendicular to q, we can determine y from energy conservation [20]:

$$\nu + M_A = \sqrt{M_N^2 + (y+q)^2} + \sqrt{M_{A-1}^2 + y^2}, \tag{2}$$

where M_A is the mass of the target nucleus and M_{A-1} is the ground state mass of the $A-1$ nucleus. In general, the scaling function depends on both y and Q^2, but at sufficiently high momentum transfer the Q^2-dependence vanishes, yielding scaling. In this PWIA analysis, the scaling function $F(y)$ can then be directly related to the nucleon momentum distribution:

$$n(k) = -\frac{1}{2\pi k} \frac{dF(k)}{dk} \tag{3}$$

This simple impulse approximation picture breaks down when the final-state interactions (FSI) of the struck nucleon with the rest of the nucleus are included. Previous calculations [21–28] suggest that the contributions from final state interactions should vanish at sufficiently high Q^2. The scaling function for Fe extracted from experiment E89-008 is shown in Fig. 2 [29]. These data show, for the first time, a clear approach to a scaling limit for heavy nuclei at large $-y$ for $Q^2 > 3$ GeV/c^2. This is shown in Fig. 3 for data from E89-008 and SLAC NE3 [1] where the Q^2 variation of $F(y)$ for several fixed values of y is shown. Note that the cross section (Fig. 4) varies over many orders of magnitude for the Q^2 range shown in the figure.

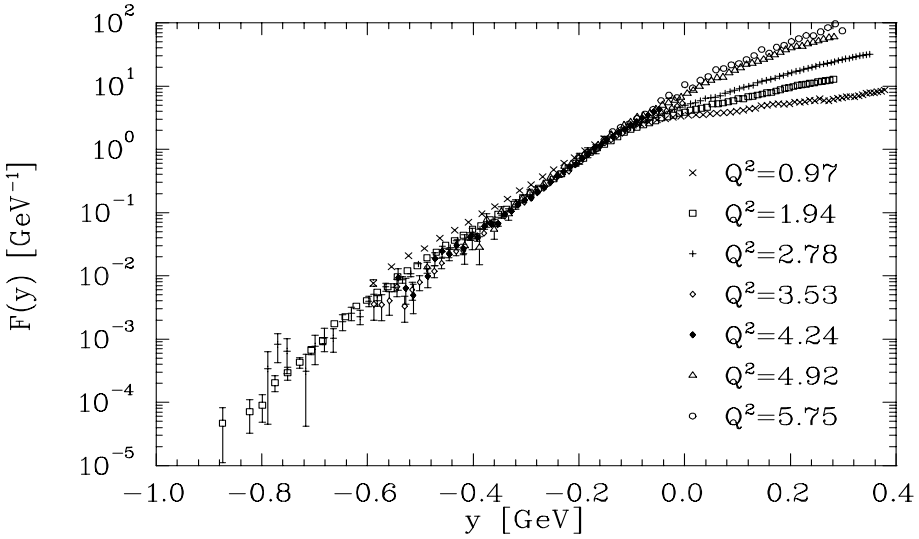

FIG. 2. Scaling function $F(y)$ for Fe from E89-008. The Q^2 values are given for Bjorken $x = 1$.

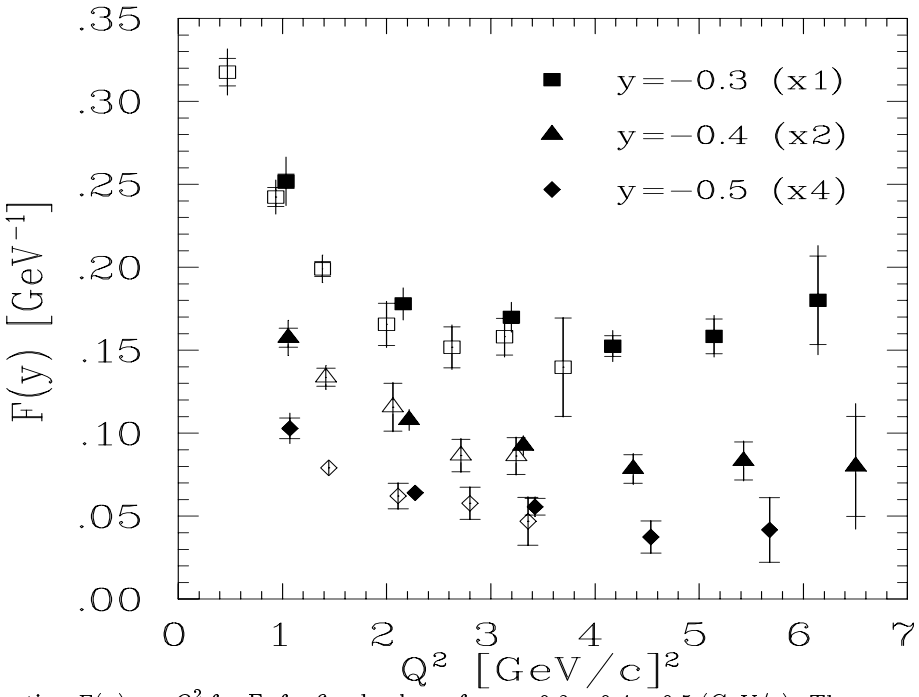

FIG. 3. Scaling function $F(y)$ vs. Q^2 for Fe for fixed values of $y = -0.3, -0.4, -0.5$ (GeV/c). The open points are calculated from the measured cross sections of the SLAC NE3 experiment. The scaling function for each value of y has been multiplied by the factors noted in parentheses.

While the observation of a scaling limit is suggestive of an approach to the impulse approximation limit, it is not definitive. Even if scaling is observed, that does not insure that the scaling function is directly connected to the momentum distribution (as we will see in the following sections). In addition, several calculations [30,31] have pointed out that while the FSI of a struck nucleon with the mean field of the rest of the nucleus is a rapidly decreasing function of Q^2, the FSI of the struck nucleon with a correlated, high-momentum nucleon may show a very weak Q^2-dependence. Experimental measurements at higher Q^2 are essential in allowing an understanding of the role of FSI in inclusive scattering. As both the large $|y|$ cross section and the high Q^2 FSI discussed above are dominated by short range nucleon-nucleon interactions, improved data at higher Q^2 may allow direct access to this interesting many-body phenomenon. The "holy grail" of these studies is to correct or eliminate FSI so that by using the impulse

approximation, the nuclear spectral function $S(p, E)$ at high values of p and E can be extracted. The region of high p includes the highly interesting regime of short range correlations (SRCs) that are expected to be present within nuclei.

While the PWIA y-scaling interpretation of the data promises the possibility to extract the nucleon momentum distribution, the possible contribution of FSIs and questions about the validity of the assumptions of the y-scaling analysis have limited the information extracted by this kind of analysis. Clearly, these data do not need to be analyzed in terms of y-scaling in order to constrain the high momentum components of the nuclear wave function. However, we will show in the following section that with only a small change to the y-scaling model, we extract a scaling function which is fully consistent with the idea that the scaling function is directly connected to the momentum distribution. This would seem to validate the assumptions of the PWIA analysis, and allow a largely model independent connection to be made between the high momentum nucleons and the modified y-scaling function.

II. RESULTS AND QUESTIONS FROM 4 GEV RUNNING

Jefferson Lab at 4 GeV offered significant improvements over previous experiments. The solid angle of the HMS as well as its large momentum acceptance allowed measurements in previously unexplored regions of x and Q^2. A program of measurements with 4 GeV beam ran in Hall C in Summer 1996, and greatly increased the x range of the available data for $1 < Q^2 < 6$ (GeV/c)^2. Cross sections were measured at seven angles and are shown in Fig. 4 for the Fe data. Data was also taken on ^{2}H, C, and Au targets. Scattered electrons were detected in the HMS and SOS spectrometers using their standard detector packages.

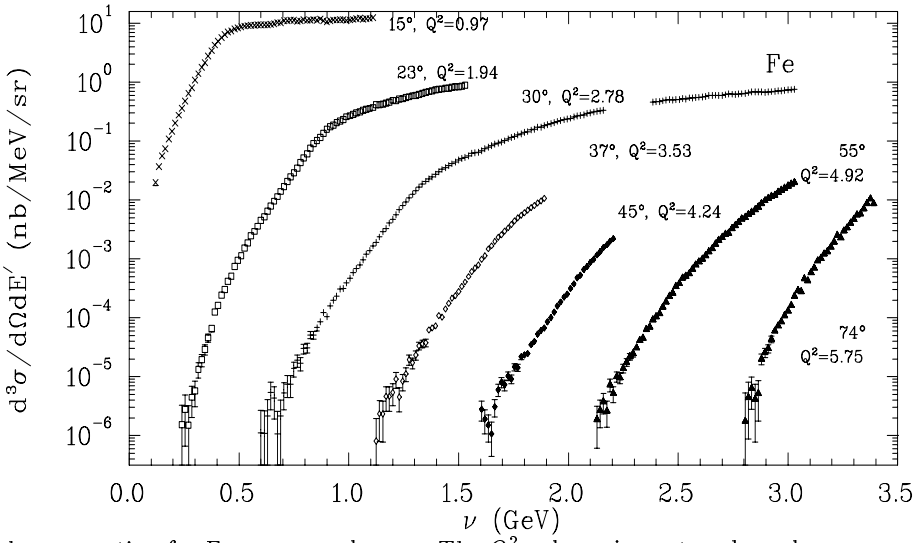

FIG. 4. Differential cross section for Fe vs energy loss, ν. The Q^2 values given at each angle correspond to Bjorken $x = 1$. Statistical errors only are shown.

Cross section were measured for all targets, and a y-scaling analysis performed. An article was published in Physical Review Letters [29] describing the inclusive scattering measurement and the analysis of in terms of the y-scaling variable. The nuclear structure function was also extracted and scaling in both Bjorken x and Nachtmann ξ have been studied. Also the Q^2-dependence of the structure function for fixed bins of x and ξ has been studied. An article was published in Physical Review C [4] presenting the structure function results. These results along with some new results will be summarized in the following sections.

While this experiment was a significant improvement over previous measurements, it was approved for just 8 days of beam time. The emphasis of the measurement was to maximize the x and Q^2 coverage on one target (Fe). Lower precision data was taken on the other nuclei. Because of this, there was not enough deuterium data at the highest x and Q^2 values to make precise comparisons between the high-x cross sections in heavy nuclei, where multi-nucleon short range correlations are believed to dominate the scattering, and the cross sections from deuterium, where the high-x components are generated entirely by two nucleon short range correlations.

A. DIS scattering, Structure Function Measurements

As was shown in Fig. 1, the structure function measured in E89-008 shows scaling in the Nachtmann variable ξ. This scaling occurs even at large values of ξ, where the scattering is dominated by resonance or even quasielastic scattering. This can be understood in terms of local duality, which leads to scaling *on average* of the proton structure function, and which leads directly to scaling for the nuclear structure function (the necessary averaging coming from the Fermi motion of the nucleons). This can also be viewed in terms of a near complete cancellation of the large higher twist contributions in the resonance region. In retrospect, it is not surprising that the nuclear structure function shows ξ-scaling in the resonance region, given the quantitative success of local duality in the proton structure function. This duality is seen if one averages over the entire resonance region or even if one averages in the region of a single resonance. However, the duality breaks down if one looks only at a fixed W^2 value (*i.e.* the top or side of a prominent resonance). Thus, the scaling in nuclei should break down where the Fermi motion is insufficient to average the proton structure function over a sufficient region. This occurs in deuterium (Fig. 5), where there is still a clear peak corresponding to the Δ resonance at low Q^2, as well as for the quasielastic peak in both deuterium and, to a lesser extent, iron (Fig. 1). However, these scaling violations are not seen for $\xi > 1$, even though we are averaging over only the low energy loss side of the quasielastic peak, and one would expect the averaging to be insufficient to invoke duality to explain the scaling. Additional data at high ξ and high Q^2 (especially for light nuclei, which provide less averaging) will allow a more careful examination of scaling in this region.

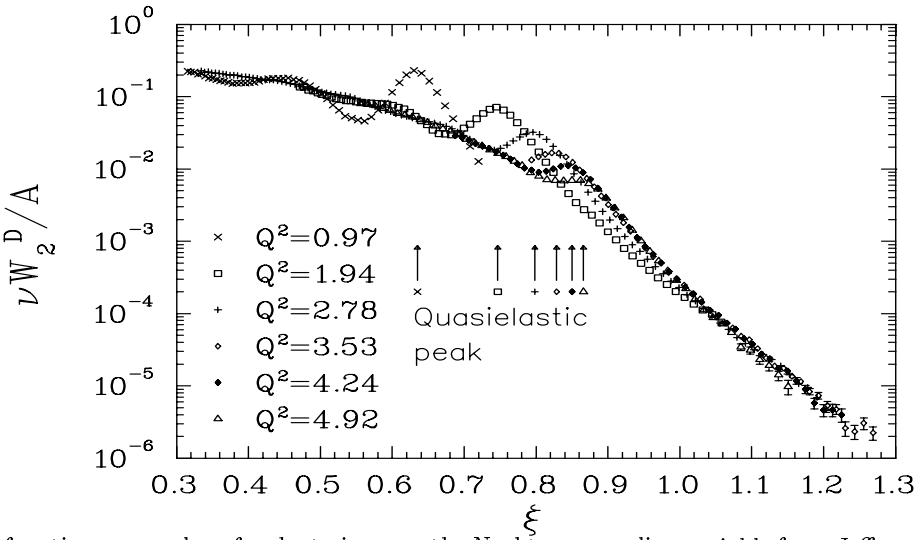

FIG. 5. Structure function per nucleon for deuterium vs. the Nachtmann scaling variable from Jefferson Lab E89-008. The Q^2 values are given for Bjorken $x = 1$. Errors shown are statistical only. The arrows indicate the position of the quasielastic peak ($x = 1$) for each data set.

This extended scaling for nuclei also means that the nuclear structure function as measured in the DIS region is the same as the structure measured at lower values of W^2. This scaling may allow measurements of the quark distributions in nuclei at lower W^2 (or equivalently lower Q^2 for fixed ξ) than accessible if one requires $W^2 > 4$ GeV^2. This may allow us to examine the ξ-dependence of the structure function for large values of ξ. This was measured at extremely high Q^2 values (~ 100 GeV^2) in $\mu-$C scattering [32] and ν-Fe scattering [33]. Near $\xi = 1$, these experiments obtained significantly different results. The neutrino experiment (CCFR) found $F_2^{Fe} \propto \exp(-8.3\xi)$, consistent with the presence of significant SRCs, and the existence of superfast quarks in the nucleus (quarks carrying a momentum greater than that of a nucleon). The muon experiment (BCDMS) found a much faster falloff $F_2^C \propto \exp(-16.5\xi)$, which does not indicate large SRC contributions. This dependence was measured for C, Fe, and Au targets by E89-008, and for all targets the dependence was in general agreement with the BCDMS measurement ($F_2^A \propto \exp(-16\xi)$). However, there are non-negligible contributions from the quasielastic peak in the vicinity of $\xi = 1$, and there is still some Q^2 variation to the structure function falloff at the largest Q^2 values from E89-008. With a 6 GeV beam, we can reach Q^2 values of 8 GeV^2 and higher for $\xi \geq 1$, where quasielastic scattering is only a small contribution to the total cross section. The QE contribution will be much smaller than in the previous experiment, so we expect that the scaling violations seen in the E89-008 data will be significantly smaller for 6 GeV running and that the extracted ξ-dependence to become independent (or at least nearly independent) of Q^2.

B. Nucleon Degrees of Freedom, $F(y)$ Measurements

While the 4 GeV data (and proposed 6 GeV extension) provide additional information on the structure function at large ξ, the main focus is the study of the momentum distribution of nucleons in nuclei, and in particular the nature of the high momentum components. The 4 GeV data from E89-008 showed y-scaling, with large Q^2-dependent scaling violations from final state interactions below $Q^2 = 3$ GeV^2 (Fig. 3). Fig. 6 shows $F(y)$ for deuterium from the 4 GeV run. While the data in the scaling region ($Q^2 > 3$ GeV^2) is limited at large y, a clear approach to scaling is observed. The solid line is a fit to $F(y)$ of the form suggested in Ref. [34]:

$$F(y) = \frac{Ae^{-a^2y^2}}{\alpha^2 + y^2} + Be^{-b|y|}. \tag{4}$$

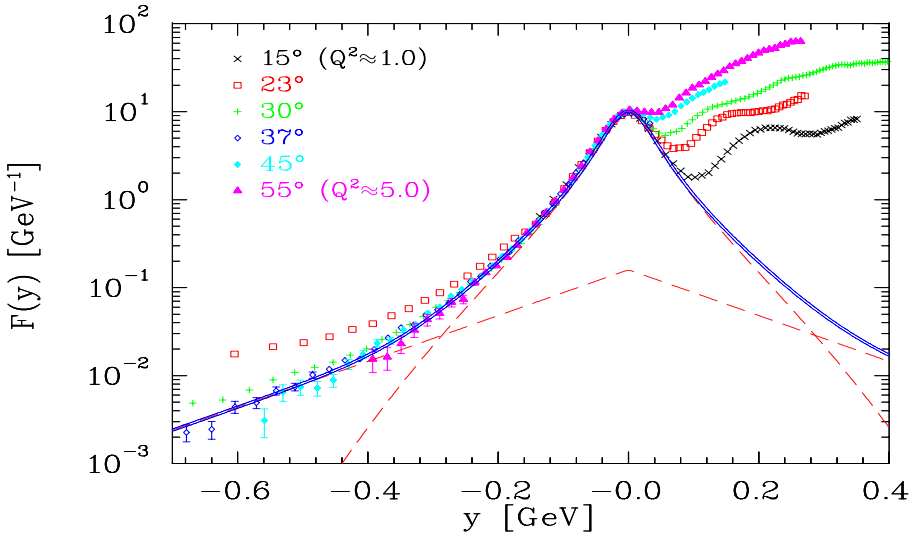

FIG. 6. Scaling function $F(y)$ for deuterium from E89-008, along with fit to data (of form given in Eq. 4).

Fig. 7 shows the momentum distribution as extracted (using Eq. 3) from the fit to $F(y)$, along with a calculation using the Argonne v14 NN potential. The agreement is quite good, even at extremely large values of $|y|$ where $n(k)$ is 4 to 5 orders of magnitude below the peak value. In particular, the slope as well as the normalization on the tail agree quite well with the calculated momentum distribution. The agreement in the tail region, which is dominated by the short range interaction of the nucleons, seems to indicate that the weakly Q^2-dependent final state interactions suggested for correlated nucleons do not make a large contribution to the scaling function. The 4 GeV data are of limited quality at the large values of y, making it difficult to extract a precise shape and normalization for this tail. Better data on deuterium, with the extended Q^2 range possible at higher energy, should allow us to extract more detailed information about the tail of the momentum distribution than we can get from the simple fit used in this analysis. A precise measurement of this region will also allow us to set significant limits on deviations from the momentum distribution due to possible weakly Q^2-dependent final state interactions of these strongly interacting (small separation) nucleons.

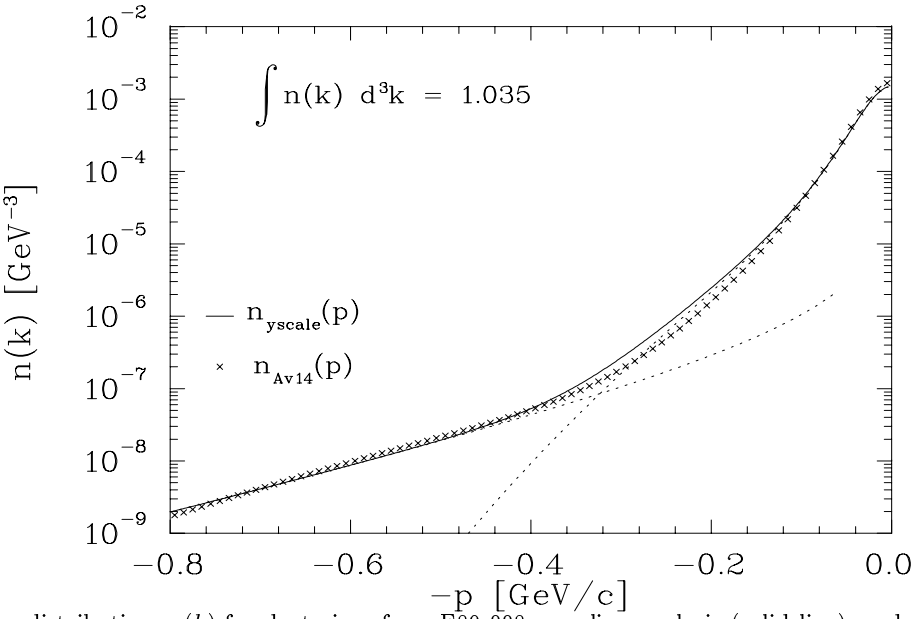

FIG. 7. Momentum distribution, $n(k)$ for deuterium from E89-008 y-scaling analysis (solid line), and calculation using the Argonne v14 potential (crosses). The dotted lines indicates the contributions of the exponential tail and the modified gaussian term from the fit to the measured $F(y)$.

While the y-scaling analysis of the deuterium data yields results consistent with exact calculations of the momentum distribution, this is not the case for the heavy nuclei. Fig. 2 shows $F(y)$ for iron. While the data show y-scaling, the falloff at large $|y|$ indicates that the high momentum components ($y \lesssim -0.5$ GeV/c) are much smaller for iron than for deuterium, even though one would expect more high momentum nucleons in the denser nuclei. This is also true for the SLAC ^{3}He data, where the extracted $F(y)$ is not consistent with calculations of the ^{3}He momentum distribution. In addition, the integral of $F(y)$ should be unity in the y-scaling picture, but the normalization of the scaling function for heavy nuclei are ∼20-30% low. For the ^{3}He data, the normalization of the scaling function has been analyzed in terms of "swelling" of the nucleon in the nucleus, and has been used to set upper limit on medium modifications to the nucleon form factors [35]. Extending such an analysis to heavier nuclei, where the normalization is even lower, would lead to a prediction of greater modifications to the nucleon radius. It is not clear that this kind of analysis gives meaningful limits on nucleon medium modifications if there is a more fundamental problem in the relation between $F(y)$ and $n(k)$. Nonetheless, tests of medium modifications from y-scaling analyses has been used to set limits on nucleon swelling used to explain the EMC effect.

The rapid falloff of the scaling function at large values of $|y|$ indicates that there is a failure of some kind in the PWIA scaling analysis. The breakdown for $A > 2$ nuclei comes from the assumption that the residual nucleus remains in an unexcited state (Eq. 2). The NN correlations responsible for much of of the high momentum components are neglected. Clearly the $(A-1)$ spectator nucleus will not be in an unexcited state if one of a pair of very high momentum nucleons is suddenly removed. The scaling violations arising from the assumption of an unexcited final state have been treated in two ways. In some cases, a correction to the scaling function is calculated, and the scaling function that is related directly to the momentum distribution is $f(y) = F(y) - B(y)$, where $F(y)$ is the measured scaling function, and $B(y)$ is the calculated binding correction. A more direct way to take the excitation of the residual nucleus into account is to determine an excitation energy for the residual system based on a modified picture of the interaction that includes the correlations. Rather than having the momentum of the struck nucleon balanced by the residual nucleus, it's momentum is balanced by a single nucleon, and the residual $(A-2)$ nucleus is at rest [36], or has a small recoil momentum [34]. We have performed an analysis of this kind using a modified definition of y, based on a simple three-body breakup of the nucleus, where the nucleon struck is assumed to be one of a correlated pair that is moving in the nucleus with a momentum (along the q vector) equal to K_{CM}. In the limit where q is much larger than the momenta of the nucleons (and thus the transverse component of these momenta can be ignored), energy conservation gives:

$$\nu + M_A = \sqrt{M_N^2 + (q + k + K_{CM}/2)^2} + \sqrt{M_N^2 + (-k + K_{CM}/2)^2} + \sqrt{M_{A-2}^2 + (-K_{CM})^2} \quad (5)$$

The scaling variable in this case is $y^* = k + K_{CM}/2$, the total initial momentum of the struck nucleon. Note that for the deuteron, there is no $(A-2)$ residual nucleus and thus no K_{CM}, so y^* is just the usual scaling variable y. Eq. 5

cannot directly be solved for y^* without a relation between y^* and K_{CM}. This is obtained by convolving the center of mass motion of the quasi-deuteron with the relative momentum of the nucleons in the pair (taken to be identical to the real deuteron momentum distribution). This allows us to determine the average K_{CM} for a given value of the initial nucleon momentum.

Fig. 8 shows the modified scaling function, $F(y^*)$, along with a fit to to $F_D(y^*)$ (dashed line). In the figure we have made a subtraction of the inelastic contribution which is significant for $y^* \gtrsim 0$. Note that the behavior at very large negative y^* is very different from the behavior in Fig. 2, and that the data is sensitive to larger values of initial nucleon momentum that one would assume based on the usual y-scaling function (probing nuclei with initial momenta of more than 1 GeV/c). However, at these very large y^* values, the uncertainties in the 4 GeV data are large, and the data just barely reach Q^2 values where scaling appears to have set in. With data at higher Q^2 values in this large y^* region, we should be able to map out the high momentum tail of the nucleon momentum distribution. Also notice that the shape of the scaling function at large negative y^* values is the same as for the deuteron, but is roughly 6 times larger (dashed line), indicating that the high momentum components appear to be well described by two nucleon correlations. This is the same behavior one sees when examining the ratio of the structure functions in the region of $1.3 \lesssim x < 2$, where the ratio is flat and roughly 5 to 6 times higher in heavy nuclei [37,15]. With better data for deuterium at large initial nucleon momenta, this comparison could be much more quantitative, and we could look for signs of high momentum components beyond the two nucleon correlations. In addition, data on ^{3}He will allow for direct comparison of high momentum nucleons ($x > 2$) in heavy nuclei to three nucleon correlations.

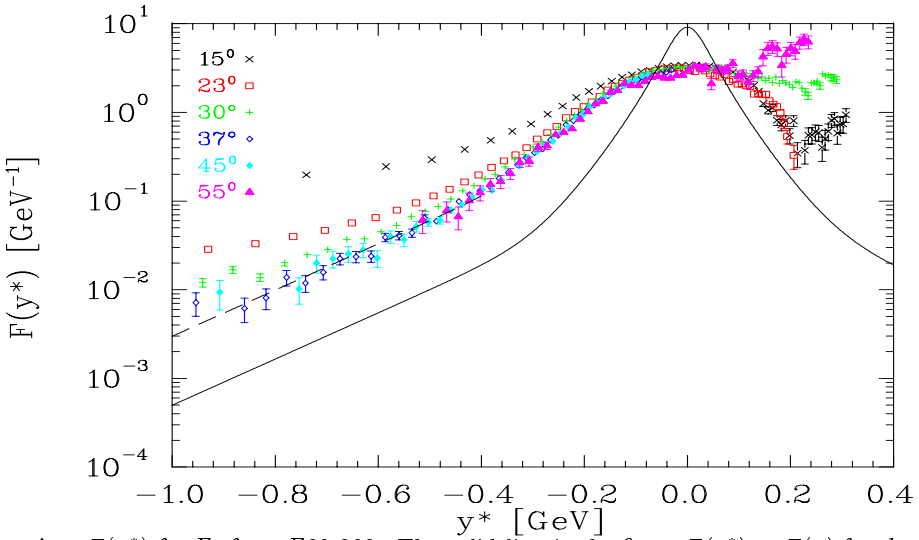

FIG. 8. Scaling function, $F(y^*)$ for Fe from E89-008. The solid line is the fit to $F(y^*) = F(y)$ for deuterium. The dashed line is the tail of the deuteron fit, scaled up by a factor of six.

Of course one does not have to rely on a non-relativistic, impulse approximation scaling analysis to study the momentum distribution and the high momentum components. One can do a complete, relativistic calculation of the cross section, using the full spectral function and including final state interactions. One can also use a relativistic scaling analysis which gives a different scaling variable and connects to light-cone momentum distributions, as suggested in Ref. [6]. The scaling analysis discussed here is intended to give a feel for the coverage and significance of the data, but also to show the success of this simple scaling analysis. This success gives us confidence in the underlying assumptions.

The question of the nature of the short range correlations can also be examined without relying on a y-scaling analysis, by directly examining the structure functions. Fig. 9 shows a calculation of the structure function per nucleon for iron, including just two nucleon correlations (solid line - from [38]), and including multinucleon correlations (dotted line - from [13]). The current data clearly indicate that the effect of multinucleon correlations is significantly smaller than estimated in the calculation. The calculation for the two nucleon SRC contributions does not include corrections for the EMC effect, but such a calculation should be available very soon [39]. The inclusion of the EMC effect will lower the calculations somewhat, making it difficult to use this data to set a strong upper limit on multinucleon components. An extension to 6 GeV will allow us to reach $Q^2 \sim 10$ GeV^2 at $x = 1.5$, where the calculation predicts very large contribution from multinucleon correlations. In addition, with data on ^{2}H, ^{3}He, and ^{4}He, it should be possible to disentangle the EMC effect from 3N correlations [39,40]. This will allow us to either obtain a clear signal

of multinucleon correlations, or set significant limits on their contributions. We can also directly compare the structure function for heavy nuclei to few body nuclei in the region where the structure function is dominated by SRCs. By comparing heavy nuclei to deuterium, we can look for deviations from the two nucleon SRCs, and by comparing to ^{3}He where the two nucleon correlations are small for $x > 2$, we can look for signatures of three nucleon correlations. This type of comparison is more direct than comparisons of the extracted momentum distribution from a scaling analysis. In addition, if there are significant final state interactions between correlated nucleons at large Q^2 values, these should cancel to first order in these ratios.

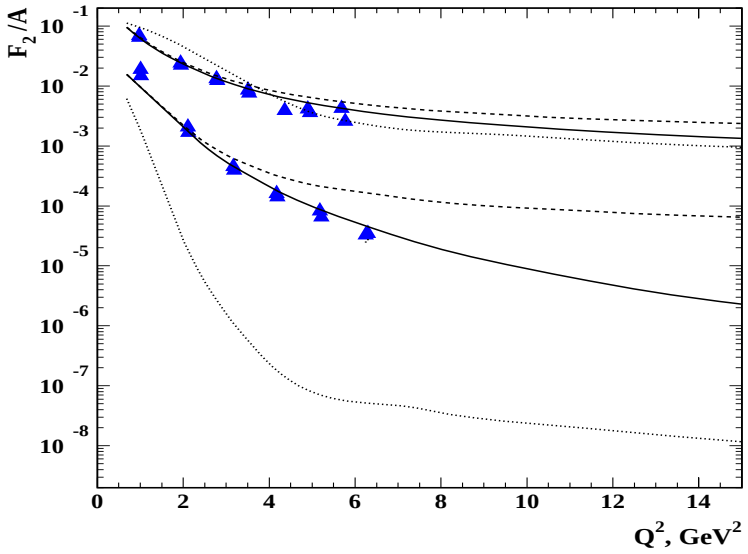

FIG. 9. Structure function for nucleon for iron from E89-008 compared to calculations without correlations (dotted lines), including two nucleon SRCs (solid lines) and multinucleon SRCs (dashed line). The upper set of data and calculations is for $x = 1$, while the lower are for $x = 1.5$.

III. DETAILS OF THE 6 GEV PROPOSED MEASUREMENTS

A. Backgrounds and Systematic Errors

We have learned a great deal from the 4 GeV running about how to improve the measurement, particularly in determining backgrounds. One source of background is the pion contamination of the electron distribution. During E89-008 this contamination was always less than 1% in the HMS when using the calorimeter and Čerenkov information for particle identification. It is estimated that during 6 GeV running this pion contamination will get somewhat worse, but is still expected to be negligible. The front two layers of the HMS calorimeter have been outfitted with phototubes on both ends of each lead glass block since the 4 GeV running was completed. This will improve our ability to distinguish electrons from pions, as will the fact that the π/e separation in the calorimeter will be better for the larger scattered electron energies of the 6 GeV kinematics.

There is also a background from secondary electrons produced in the target which was larger than expected for E89-008. The main source likely comes from electro-production and photo-production of neutral pions. These pions then decay into photons which can produce positron-electron pairs. This background is charge-symmetric, and can be measured directly by changing the spectrometer to positive polarity and detecting the produced positrons. For the largest angles measured in E89-008 (55° and 74°), this background was significant and required a fit to our positron measurements and subtraction from our electron data (see Ref. [41] for more details). As a result, we will limit our running with 6 GeV beam to 60°, and have included time in our beamtime request to measure this background.

The combined systematic uncertainties from the E89-008 run totaled 3.2 to 4.7% for the HMS data with the primary contributors being knowledge of the acceptance, radiative corrections, target thickness, and bin centering (correcting an integral number of counts within a momentum/angle bin to the measured cross section at the center of the bin). Each of these four items ranged from approximately 1% to 2% depending on the scattering angle. Table 1 below from

Ref. [41] summarizes the systematic uncertainties during the 4 GeV running. We expect similar results for the 6 GeV running.

There is an additional uncertainty in the extraction of F_2 from the cross section due to the uncertainty in $R = \sigma_L/\sigma_T$. This was generally negligible, except at the largest x and Q^2 values measured. We will take a small amount of data with ~ 4 GeV beam, both as a cross calibration with the previous measurement and also to provide a rough determination of R. In the E89-008 analysis, a value of $R = 0.32/Q^2$ was assumed, with a 100% uncertainty in this value. At the highest Q^2 possible with 6 GeV measurements, it is not clear if this uncertainty is large enough. We expect to be able to measure R at relatively high values of Q^2 (where R is quite small) with uncertainties of $50-100\%$, which will be sufficient to keep this from being a dominant source of uncertainty in the extracted structure functions.

TABLE I. Systematic uncertainties in the extraction of the cross section for 4 GeV running. Entries with an asterisk indicate that a correction was made directly to the cross section which had the listed uncertainty. Entries without an asterisk indicate no correction to the cross section, just a contribution to the overall uncertainty.

Systematic	HMS
Acceptance Correction	1.0-2.2%*
Radiative Correction	2.5%*
Target Track Cuts	0.5%
Bin Centering Correction	1.0-2.2%*
PID Efficiency	0.5%*
Charge Measurement	1.0%
Target Thickness	0.5-2.0%
Target/Beam Position Offset	0.25%
Tracking Efficiency	0.5%*
Trigger Efficiency	0.05%*
Normalization	0.0%
COMBINED UNCERTAINTY	3.2-4.7%

B. Proposed Kinematics with 6 GeV Beam

Fig. 10 shows the kinematic range in x and Q^2. The region below the dashed (solid) curve is what is accessible with 4 (6) GeV beam at JLab ($\theta \leq 60^\circ$ in both cases). Experiment E89-008 did not cover the full Q^2 range for very large x values, so the existing data for $x > 2.2$ is limited to $Q^2 \lesssim 3.5$ GeV^2. Previous SLAC measurements of inclusive electron scattering from nuclei [1] were limited to $x \leq 3$ and $Q^2 \leq 3$ (GeV/c)^2. The same measured cross sections will then be examined as a function of the scaling variable y and Q^2. Fig. 11 shows the kinematic range in y and Q^2. Again, the dashed curve is what can be measured with 4 GeV beam, and the solid curve represents the coverage available with a 6 GeV beam. An addition to the measurement since the original proposal in 1994 is the inclusion of ^{3}He and ^{4}He cryogenic targets. The proposed data will significantly increase the Q^2 coverage for ^{3}He and ^{4}He compared to earlier SLAC measurements [42,1].

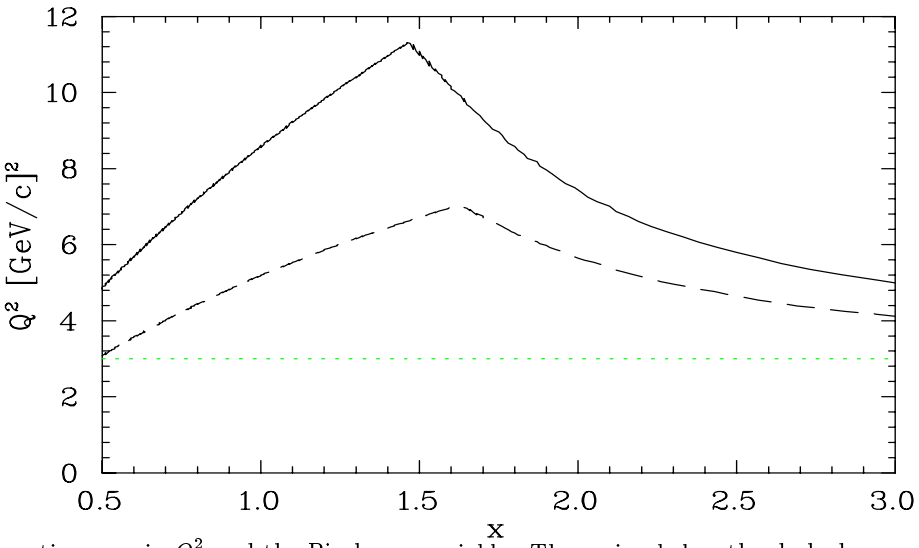

FIG. 10. The kinematic range in Q^2 and the Bjorken x variable. The region below the dashed curve is the range of data accessible with 4 GeV beam, and the region below the solid curve and indicates the range possible with a 6 GeV beam. The dotted line indicates the approximate Q^2 value where ξ-scaling is observed in the previous data. Experiment E89-008 did not cover the entire Q^2 range accessible at extremely large x values ($x > 2$) so the current data for these large values of x are limited to ~ 3.5 GeV^2 (just barely in the region where scaling is observed).

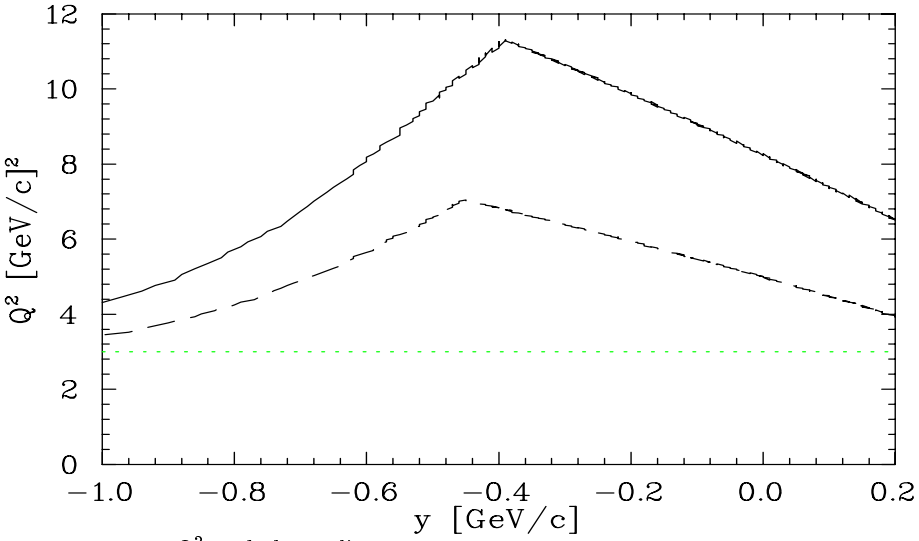

FIG. 11. The kinematic range in Q^2 and the scaling variable y. The dashed curve indicates the coverage available with 4 GeV beam and the solid curve and the dashed curve indicates the increased range possible with a 6 GeV beam. The dotted line indicates the approximate Q^2 value where y-scaling is observed in the previous data.

The increase in beam energy to 6 GeV will have the greatest impact on the Q^2 range for kinematic points with $1.0 \lesssim x \lesssim 1.7$. This extended Q^2 data is critical to studies of the transition from scattering from nucleons to scattering from quarks as described in the introduction. At larger values of x, the Q^2 increase is smaller, but is crucial for studies of the nature of the short range correlations. While the Q^2 increase is not as large as for the lower x values, it is enough to allow us to reach well into the scaling region ($Q^2 \gtrsim 3$ GeV^2) out to extremely large x values. The 4 GeV measurement only reached $Q^2 \approx 3.5$ GeV^2 for $x > 2.2$, and while the Q^2 coverage for iron was much better for $1.5 < x < 2$, the deuterium data in this region was quite limited. The increased Q^2 range for large x corresponds to a similar increase in Q^2 for large negative values of y allowing direct study of the approach to the scaling limit, as well as data in the scaling region for extremely large values of $|y|$. This high x (large negative y) region is very important in determining if the high momentum components are explained by two nucleon correlations or if large multinucleon correlations are required.

A beam energy of 6 GeV is sufficient to reach the scaling limit for the highest values of x (≈ 3), and energies above 6 GeV do not significantly improve the Q^2 coverage for these very large values of x. Higher beam energies would have the most improvement in kinematic coverage for $x < 1.5$. However, the higher Q^2 values accessible in that x region are not necessary for probing nucleon momentum distributions and short range correlations. One may be able to perform "DIS" experiments for $x \gtrsim 1$ at extremely high Q^2 values (where the quasielastic and resonance contributions will disappear even for $x > 1$). Such an experiment would require energies well above 6 GeV. Thus, we feel that 6 GeV is the most appropriate energy for the proposed measurement.

C. Experimental Equipment

The experimental set-up for measurements with a 6 GeV beam would be essentially the same as used for the 4 GeV measurements. No new detectors would be needed. Data would be taken in the HMS spectrometer using a detector package including a threshold gas Čerenkov counter and a lead glass shower counter for rejection of pion background. Several nuclear targets (C, Cu, and Au) would be used as well as cryogenic targets. We will run at beam currents between 20 and 80 μA. While the kinematics below are calculated for a 6 GeV beam energy, we will run at whatever maximum energy is available when the experiment is scheduled. Any energy above 5.5 GeV would be acceptable, although there is an improvement in kinematic coverage if slightly higher beam energies are available.

A cryogenic hydrogen target is necessary for calibration and a cryogenic deuterium target for production data. These are currently part of the standard Hall C cryotarget system. ^{3}He cells have been used for pion and kaon electroproduction experiments in Hall C, and a ^{4}He target was used in 1999 for a kaon electroproduction measurement. Since there are other approved experiments in Hall C that will use helium targets, we assume that they will be available and will take beam currents at least as high as previous Hall C measurements (30-40 μA).

The measurements would be done at several angles to cover the full kinematic range. Table II is a list of estimated running times for six angle settings between $\theta = 20^\circ$ and 60°. The assumptions are 60 μA of beam current (40μA for the helium targets), a spectrometer solid angle of 7 msr, a momentum bite of 16%, a fixed x bin of 0.05, and a maximum statistical error of 10%. The majority of the data will be taken in the HMS. The SOS will take some additional data at the largest angles, as well as make measurements of the pion and charge-symmetric electron/positron background.

IV. REQUEST TO LABORATORY

We request approval to extend the measurements of inclusive scattering from nuclei at $x > 1$ and high Q^2 with a 6 GeV beam at Jefferson Lab. We will take data on three solid targets, focussing mainly on C and Cu, but also taking data on Au at a limited set of Q^2 values. We have replaced the iron target used in E89-008 with copper in order to run at higher currents. The combined time for data taking on these targets is 180 hours. We will also take data on deuterium, ^{3}He, and ^{4}He (focussing on deuterium and ^{3}He), for a combined running time of 270 hours. The kinematics below 40° are chosen to optimize the Q^2 coverage for the large x data, while the large angle data will give the maximum Q^2 range for $1.3 \lesssim x \lesssim 1.7$.

Check-out and commissioning time is estimated to require 20 hours, hydrogen elastic running an additional 25 hours, cross calibration to E89-008 with a 4 GeV beam (and a limited L/T separation) will require approximately 40 hours. Special runs to measure backgrounds (positron background and empty target runs) will require approximately 40 hours. The sum time for check-out, calibration, and background measurements is 125 hours. The average overhead for configuration changes will vary from approximately 15 minutes to 1 hour depending on the target changes involved

and whether the magnet polarity will be changed. We estimate a total of 100 hours of overhead time for configuration changes.

Our total beam time request, including checkout, background measurements, and data taking on six targets is 675 hours, or approximately 28 beam days.

TABLE II. Kinematics of the proposed experiment for 6 GeV running.

θ (deg)	E' (GeV)	x_{range}	y_{min} (GeV/c)	Q^2_{range} $(\mathrm{GeV/c})^2$	time(hrs) C+Cu+Au	time(hrs) D+^{3}He+^{4}He
20.0	3.9-5.3	0.7-3.0	-1.0	2.5-3.9	18	27
25.0	3.2-4.7	0.7-2.5	-0.8	3.5-4.9	24	36
30.0	2.7-4.1	0.7-2.0	-0.7	3.5-6.8	33	48
40.0	1.9-3.0	0.7-1.7	-0.5	4.0-8.9	42	63
50.0	1.4-2.1	0.7-1.5	-0.4	4.4-9.8	42	63
60.0	1.1-1.8	0.7-1.4	-0.4	4.5-10.8	21	33

V. SUMMARY

We propose to measure inclusive scattering at $x > 1$ on several light and heavy nuclei. The experiment will measure the cross section in the y-scaling region ($Q^2 \gtrsim 3$ GeV^2) over a large y range, (corresponding to values of x up to $x \approx 3$). This data is sensitive to the nucleon momentum distribution, and in particular to the high momentum components of the nucleon distribution in nuclei (probing nucleons with initial momenta in excess of 1000 MeV/c). By comparison to calculations of nuclear structure, or by direct comparisons of heavy nuclei to ^{2}H and ^{3}He, we will study the nature of the high momentum components to determine to what extent two nucleon correlations explain the presence of very high momentum nucleons and to what extent multinucleon correlations are required.

This data will complement the many completed and upcoming coincidence $A(e,e'p)$ and $A(e,e'NN)$ measurements attempting to probe the high momentum components of the spectral function and short range correlations [43]. The inclusive measurement can reach much larger values of the missing momentum, where the coincidence measurements become cross section (or background) limited. The inclusive measurements are also cleaner, being significantly less sensitive to final state interactions, meson exchange currents, and other processes which must be modeled in the analysis of the coincidence measurements. In the inclusive measurement, one does not reconstruct the excitation energy of the final system (the missing energy of the struck nucleon), and so is sensitive to the entire missing energy distribution of the spectral function. Both inclusive and coincidence experiments are important in these studies, as inclusive measurements can provide fairly clean information on the very high momentum components of the spectral function, while the coincidence experiments can provide detailed information on the missing energy distribution (and momentum distributions for the individual shells) at lower momentum values.

In addition to the main goal of studying nucleon distributions and short range correlations in nuclei, this data will also allow us to extract the nuclear structure functions at large x values. This will allow us to extend measurements of duality and scaling in nuclei, especially for $\xi > 1$ where it is not clear that ξ-scaling is a natural consequence of local duality. In addition, measurements of the structure function in nuclei at large values of x will significantly improve the extraction of nuclear moments when combined with precision data in the deep inelastic and resonance region that will be taken in future JLab experiments [10,11].

[1] D. B. Day *et al.*, Phys. Rev. Lett. **59**, 427 (1987).
[2] B. W. Filippone *et al.*, Phys. Rev. **C45**, 1582 (1992).
[3] J. Arrington *et al.*, Phys. Rev. **C53**, 2248 (1996).
[4] J. Arrington *et al.*, Phys. Rev. **C64** 014602 (2001).
[5] O. Benhar and S. Liuti, Phys. Lett. **B358**, 173 (1995).
[6] S. Simula, arXiv:nucl-th/0002030 (2001).
[7] E. Bloom and F. Gilman, Phys. Rev. **D4**, 2901 (1971).
[8] I. Niculescu *et al.*, Phys. Rev. Lett. 85, 1186 (2000); I. Niculescu, Ph.D. Thesis, Hampton University (1999).
[9] C. S. Armstrong, R. Ent, C. E. Keppel, S. Liuti, G. Niculescu and I. Niculescu, Phys. Rev. **D63** 094008 (2001).
[10] C. E. Keppel *et al.*, JLab Experiment E97-010, (1997); I. Niculescu *et al.*, JLab Experiment E00-002 (2000).
[11] J. Arrington *et al.*, JLab Experiment E00-101, (2000).
[12] D. Day *et al.*, Ann. Rev. Nucl. Part. Sci. **40**, 357 (1990).
[13] L. L. Frankfurt and M.I. Strikman, Phys. Lett. **B94** 216 (1980)
[14] C. C. degli Atti and S. Simula, Phys. Lett. **B325**, 276 (1994).
[15] O. Benhar, A. Fabrocini, S. Fantoni, and I. Sick, Phys. Lett. **B343** 47 (1995).
[16] G. B. West, Phys. Rep. **18**, 263 (1975).
[17] Y. Kawazoe, G. Takeda and H. Matsuzaki, Prog. Theo. Phys. **54**, 1394 (1975).
[18] T. DeForest, Nucl. Phys. **A392**, 232 (1983).
[19] M. Gari and W. Krümpelmann, Phys. Lett. **B141**, 295 (1984).
[20] E. Pace and G. Salmé, Phys. Lett. **B110**, 411 (1982).
[21] B. L. Ioffe, V. Khoze, and L. N. Lipatov, **Hard Processes** (Horth-Holland, Amsterdam, 1984).
[22] E. Pace, G. Salmé, and G. B. West, Phys. Lett. **B273**, 205 (1991).
[23] O. Benhar *et al.*, Phys. Rev. **C44**, 2328 (1991).
[24] O. Greenberg, Phys. Rev. **D47**, 331 (1993).
[25] B. L. Ioffe, ZhEFT Lett. **58**, 930 (1993).
[26] E. Pace, G. Salmé, and A. S. Rinat, Nucl. Phys. **A572**, 1 (1993).
[27] S. A. Gurvitz and A. S. Rinat, Phys. Rev. **C47**, 2901 (1993).
[28] A. S. Rinat and M. F. Taragin, Nucl. Phys. **A620**, 417 (1997). Erratum: Nucl. Phys. **A624**, 773 (1997).
[29] J. Arrington *et al.*, Phys. Rev. Lett. **82**, 2056 (1999).
[30] C. C. degli Atti and S. Simula, Phys. Lett. **B325** 276 (1994).
[31] O. Benhar, Private Communication (1998).
[32] A. C. Benvenuti *et al.* [BCDMS Collaboration], Z. Phys. **C63**, 29 (1994).
[33] M. Vakili *et al.* [CCFR Collaboration], Phys. Rev. **D61**, 052003 (2000).
[34] C. C. degli Atti and G. B. West, Phys. Lett. **B458**, 447 (1999).
[35] R. D. McKeown, Phys. Rev. Lett. **56** 1452 (1986).
[36] Xiangdong Ji and R. D. McKeown, Phys. Lett. **B236**, 130 (1990).
[37] L. L. Frankfurt, M. I. Strikman, D. B. Day, and M. M. Sargsian, Phys. Rev. **C48** 2451 (1993).
[38] L. L. Frankfurt, D. B. Day, M. M. Sargsian, and M. I. Strikman, Phys. Rev. **C48**, 2451 (1993).
[39] M. M. Sargsian, Private Communication (2001).
[40] M. I. Strikman, Private Communication (2001).
[41] J. Arrington, Ph.D. Thesis, Caltech, www.jlab.org/∼johna/thesis (1998).
[42] S. Rock, *et al.*, Phys. Rev. **C26** 1592 (1982).
[43] W. Hersman *et al.*, JLab experiment E89-031 M. Epstein *et al.*, JLab experiment E89-044; I. Sick, *et al.*, JLab experiment E97-006; J. A. Templon *et al.*, JLab Experiment E97-111; A. Saha *et al.*, JLab Experiment E00-102; W. Bertozzi *et al.*, JLab experiment E01-015; K. Aniol *et al.*, JLab experiment E01-108